Supplementary Methods and Results Empowering the crowd: Feasible strategies to minimize the spread of COVID-19 in informal settlements

Alberto Pascual-García[1,*], Jordan Klein[2], Jennifer Villers[3,∧], Eduard Campillo-Funollet[4,∧], Chamsy Sarkis[5]

August 26, 2020

(1) Institute of Integrative Biology. ETH-Zürich. Zürich, Switzerland.
(2) Office of Population Research. Princeton University. Princeton, NJ, USA.
(3) Princeton Environmental Institute. Princeton University. Princeton, NJ, USA.
(4) Genome Damage and Stability Centre. University of Sussex. Brighton, United Kingdom.
(5) Pax Syriana Foundation. Valetta, Malta.
(∧) Equal contribution.
(*) correspondence: alberto.pascual@env.ethz.ch

Model

We consider a stochastic model governed by the following set of differential equations:

$$\dot{S}_i = -\lambda_i S_i \tag{1}$$
$$\dot{E}_i = \lambda_i S_i - \delta_{\mathrm{E}} E_i \tag{2}$$
$$\dot{P}_i = \delta_{\mathrm{E}} E_i - \delta_{\mathrm{P}} P_i \tag{3}$$
$$\dot{A}_i = (1-f)\delta_{\mathrm{P}} P_i - \gamma_{\mathrm{A}} A_i \tag{4}$$
$$\dot{I}_i = f\delta_{\mathrm{P}} P_i - ((1-g_i-h_i)\gamma_I + h_i\eta + g_i\alpha) I_i \tag{5}$$
$$\dot{H}_i = h_i \eta I_i - \gamma_{\mathrm{H}} H_i \tag{6}$$
$$(\dot{R/D})_i = \gamma_{\mathrm{H}} H_i \tag{7}$$
$$\dot{R}_i = \gamma_{\mathrm{A}} A_i + (1-g_i-h_i)\gamma_{\mathrm{I}} I_i \tag{8}$$
$$\dot{D}_i = g_i \alpha I_i \tag{9}$$

where

$$\lambda_i = \sum_{j=1}^{n} \beta_{ij} \frac{P_j + A_j + I_j + H_j}{N_j} \tag{10}$$

with $\beta_{ij} = \tau C_{ij}$, where τ is the probability of infection if there is a contact between a susceptible and an infected person, and C_{ij} is the average number of contacts of an individual of class i with an individual of class j per day. The model is illustrated in Fig. 1, and the rest of the parameters are described in Tables 1 and 2.

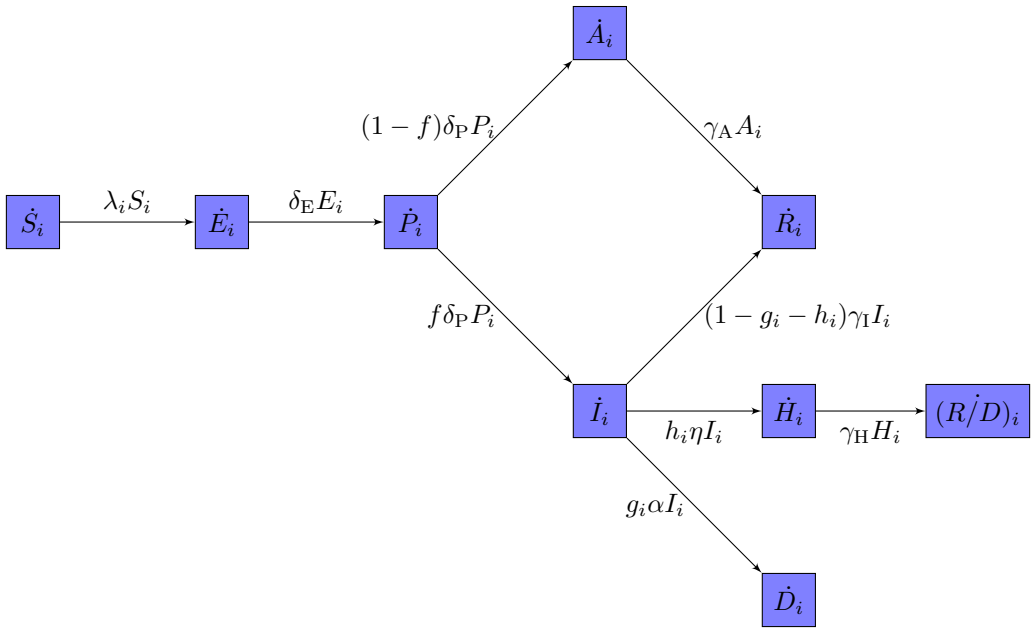

Figure 1: **Diagram of the model.** The model considers the following compartments: susceptible (S), exposed (E), infectious-presymptomatic (P), infectious-asymptomatic (A), infectious-symptomatic (I), infectious-requiring hospitalization (H), recovered (R) and dead (D). Our model considers 3 potential outcomes for symptomatic cases (I): mild cases will recover (R) after the typical infectious period, severe cases will have an extended infectious period during which they require hospitalization (H), and critical cases requiring ICU care will die (D) after the symptomatic period. Since the fate of individuals in the H compartment is uncertain if healthcare is not available, we run simulations considering two possibilities: either all recover, or all die, represented by the R/D compartment.

Population structure and model parameters

Table 1: **Population structured parameters.**

Population class	Age 1 (0-12)	Age 2 (13-50), no comorbidities	Age 2 (13-50), comorbidities	Age 3 (>50), no comorbidities	Age 3 (>50), comorbidities	References
Fraction in class	.407	.471	.0626	.022	.0373	[1, 2, 3]
h_i	.064	.067	.199	.183	.445	[4, 5]
g_i	.0065	.02	.094	.063	.222	[4, 5]
$\bar{c}_i$,	25	15	15	10	10	From camp managers

In April, 2020, 40.7% of the population in informal IDP camps in Northern Syria was aged 0-12, 53.4% aged 13-50, and 5.9% aged 51+ [3]. To estimate the proportion of each age group with comorbidities, we calculated the weighted average age-specific comorbidity prevalence of the 4 most common comorbidities in the Syrian refugee populations in Jordan and Lebanon: hypertension, cardiovascular disease, diabetes, and chronic respiratory disease [2, 1]. We standardized these weighted averages to the age structure of IDPs in Northern Syria and estimated that 11.7% of people aged 13-50 have comorbidities, while 62.9% of people aged 51+ have comorbidities.

We estimated the fractions of symptomatic cases in children aged <13 that would become severe and critical from the fractions of symptomatic cases in children aged <11 that were severe and critical in China [4]. We estimated the class-specific fractions of symptomatic cases in adults that would become severe and critical using the age and comorbidity-specific fractions of symptomatic cases with known outcomes that required hospitalization, without and with ICU admission, respectively in the United States [5]. To account for poorer health among Syrian adults

compared to their similarly aged peers in developed countries, estimates for US adults aged 19-64 were used for Syrian adults aged 13-50, while estimates for US adults aged 65+ were used for Syrian adults aged 51+.

Table 2: **Model parameters.**

Parameter	Description	Value	Distribution	Reference
$1/\delta_E + 1/\delta_P$	Incubation period (days)	5.2 (95% CI: 4.1-7.0)	Lognormal	[6]
$1/\delta_P$	Presymptomatic infectious period (days)	2.3 (95% CI: 0.8-3.8)	Gaussian	[7, 8]
$1/\delta_E$	Latent period (days)	$(1/\delta_E + 1/\delta_P) - 1/\delta_P$ (Minimum = .5 days)		Derived
$1/\gamma_I$	Symptomatic infectious period (days)	7	---	[7, 9]
$1/\gamma_A$	Asymptomatic infectious period (days)	7	---	[7, 9]
$1/\eta$	Time from symptom onset to requiring hospitalization (days)	7 (IQR: 4-8)	Gamma	[10]
$1/\alpha$	Time from symptom onset to death (critical cases, days)	10 (IQR: 6-12)	Gamma	[10]
$1/\gamma_H$	Time from requiring hospitalization to recovery/death (days)	10 (IQR: 7-14)	Gamma	[10]
f	Probability an infectious individual is symptomatic	0.84 (95% CI: 0.8-0.88)	Binomial	[11]
h_i	Fraction of symptomatic cases severe	Age and comorbidity-dependent (see Table 1)	---	[4, 5]
g_i	Fraction of symptomatic cases critical	Age and comorbidity-dependent (see Table 1)	---	[4, 5]
---	Reduction in probability of infection from contact in buffer zone	80%	---	Assumed

To estimate the latent period ($1/\delta_E$), we calculated the difference between randomly generated incubation ($1/\delta_E + 1/\delta_P$) and presymptomatic ($1/\delta_P$) periods. We estimated the presymptomatic period using results reported by He et al. [7] and found they best fit a Gompertz distribution with a mean of 2.3 days (95% CI: 0.8-3.0). Since a correction of these by Ashcroft et al. [8] suggests they significantly underestimate the presymptomatic period's upper bound, we estimated that the true presymptomatic period follows a Gaussian distribution around the mean (95% CI: 0.8-3.8). However, this presymptomatic period distribution implies a non-negligible probability of a negative latent period. To correct this discrepancy, we assumed a minimum latent period of .5 days [12]. Time from symptom onset to death in critical cases ($1/\alpha$) is estimated using time from symptom onset to ICU admission in Wang et al [10].

Table 3: **Fraction of population in each zone by safety zone scenario.**

Scenario	Age 1, orange	Age 1, green	Age 2 no comorbidities, orange	Age 2 no comorbidities, green	Age 2 comorbidities, orange	Age 2 comorbidities, green	Age 3 no comorbidities, green	Age 3 comorbidities, green
Only age 3 in green zone	.407	0	.471	0	.0626	0	.022	.0373
Age 3 + age 2 with comorbidities in green zone	.407	0	.471	0	0	.0626	.022	.0373
20% green zone capacity	.376	.0312	.424	.0469	0	.0626	.022	.0373
25% green zone capacity	.356	.0512	.394	.0769	0	.0626	.022	.0373
30% green zone capacity	.336	.0712	.364	.107	0	.0626	.022	.0373

We explore different scenarios for allocating members of each population class to the safety, or "green" zone, and the exposed, or "orange" zone. In one scenario, we only place individuals in age group 3 (>50) in the green zone, while in another we place all vulnerable individuals, age group 3 and age group 2 (13-50) with comorbidities, in the green zone. In 3 additional scenarios, after all vulnerable individuals are allocated to the green zone, we set the green zone's capacity to a certain percentage of the camp's population (20%, 25%, 30%), and allocate its remainder to non-vulnerable family members, who by necessity are either children <13 in age group 1 or healthy younger adults in age group 2. In accordance with camp managers' expectations that many vulnerable individuals will have non-vulnerable spouses, while fewer vulnerable individuals will have young children, in these scenarios we allocate 40% of the remainder of the green zone to children and 60% of the remainder of the green zone to younger adults without comorbidities. We also consider a baseline scenario in which there is no green zone.

Parameterization of the contact matrix

We estimated the average number of contacts that individuals of class i have in a camp, $\bar{c}_i$ (see Table 1), and we parameterized the contact matrix assuming that, in a well-mixed population, these contacts will be distributed among classes relative to the fraction of individuals within each class, i.e.

$$C^0_{ij} = \bar{c}^0_i N_j / N, \tag{11}$$

with N the total population size and N_j the population size of class j. A well-mixed population will be considered the null model, and parameters derived under the null model assumptions are indexed with the superscript 0, e.g. the null contact matrix is C^0_{ij}. Some of the interventions we considered either reduce the average number of contacts of class i (e.g. self-isolation) or the probability that individuals of class i interact with those of class j (e.g. safety zone strategies). We model the first type of intervention introducing the parameter ϵ_{ij}, representing the fraction of the average number of contacts observed in the null model that prevail after the intervention: $\bar{c}_i = \epsilon_i \bar{c}^0_i$. Similarly, we model the second type of intervention with the matrix m_{ij}, representing the fraction of population j visible to population i after the intervention. The contact matrix resulting from management strategies can therefore be written with respect to the null model as:

$$C_{ij} = \epsilon_i m_{ij} \bar{c}^0_i N_j / N = \epsilon_i m_{ij} C^0_{ij} = M_{ij} C^0_{ij}. \tag{12}$$

We name the matrix M_{ij} the management matrix. Substituting Eq. 12 in the explicit expression of λ (Eq. 10) yields a general expression for management strategies acting on the contact matrix:

$$\lambda_i = \frac{\tau}{N} \sum_{j=1}^{n} \epsilon_{ij} \bar{c}_i^0 m_{ij} \left(P_j + A_j + I_j + H_j\right) \tag{13}$$

Derivation of the transmissivity parameter τ

Estimation of the Next Generation Matrix

In the following, to simplify the notation we define $\kappa_i = ((1 - g_i - h_i)\gamma_{\mathrm{I}} + h_i\eta + g_i\alpha)$. To estimate the probability of infection if there is a contact between a susceptible and an infected individual (parameter τ) we proceed as follows [13, 14, 15]. We start by considering the subsystem containing the infected population:

$$\dot{E}_i = \lambda_i S_i - \delta_{\mathrm{E}} E_i \tag{14}$$

$$\dot{P}_i = \delta_{\mathrm{E}} E_i - \delta_{\mathrm{P}} P_i \tag{15}$$

$$\dot{A}_i = (1 - f)\delta_{\mathrm{P}} P_i - \gamma_{\mathrm{A}} A_i \tag{16}$$

$$\dot{I}_i = f\delta_{\mathrm{P}} P_i - \kappa_i I_i \tag{17}$$

$$\dot{H}_i = h_i \eta I_i - \gamma_{\mathrm{H}} H_i. \tag{18}$$

For the sake of simplifying the notation, let us consider the following ordering of the variables in the vector $x = (E_1, ..., E_{\mathrm{M}}, P_1, ..., P_{\mathrm{M}}, A_1, ..., A_{\mathrm{M}}, I_1, ..., I_{\mathrm{M}}, H_1, ..., H_{\mathrm{M}})$, with M the number of population classes. We are interested in the parameterization of the null model, which will serve as a baseline to estimate the parameter τ, which is initially unknown, but does not change when interventions are introduced. For the null model, Eq. 13 becomes

$$\lambda_i = \frac{\tau}{N} \sum_{j=1}^{n} \bar{c}_i^0 \left(P_j + A_j + I_j + H_j\right).$$

Following this notation, the linearized system can be written in the form $\dot{\boldsymbol{x}} = (\boldsymbol{T} + \boldsymbol{\Sigma})\boldsymbol{x}$, where:

$$\boldsymbol{T} = \tau \begin{bmatrix} \mathbf{0} & \boldsymbol{\Theta} & \boldsymbol{\Theta} & \boldsymbol{\Theta} & \boldsymbol{\Theta} \\ \mathbf{0} & \mathbf{0} & \mathbf{0} & \mathbf{0} & \mathbf{0} \\ \mathbf{0} & \mathbf{0} & \mathbf{0} & \mathbf{0} & \mathbf{0} \\ \mathbf{0} & \mathbf{0} & \mathbf{0} & \mathbf{0} & \mathbf{0} \\ \mathbf{0} & \mathbf{0} & \mathbf{0} & \mathbf{0} & \mathbf{0} \end{bmatrix} \tag{19}$$

is the transmission matrix, with $\boldsymbol{\Theta} = \mathrm{diag}(p_i \bar{c}_i^0)\boldsymbol{U}$, $p_i = N_i/N$, and $\boldsymbol{U}$ is the all ones matrix of size M. The transition matrix is

$$\boldsymbol{\Sigma} = \begin{bmatrix} -\delta_{\mathrm{E}}\boldsymbol{I} & \mathbf{0} & \mathbf{0} & \mathbf{0} & \mathbf{0} \\ \delta_{\mathrm{E}}\boldsymbol{I} & -\delta_{\mathrm{P}}\boldsymbol{I} & \mathbf{0} & \mathbf{0} & \mathbf{0} \\ \mathbf{0} & (1-f)\delta_{\mathrm{P}}\boldsymbol{I} & -\gamma_{\mathrm{A}}\boldsymbol{I} & \mathbf{0} & \mathbf{0} \\ \mathbf{0} & f\delta_{\mathrm{P}}\boldsymbol{I} & \mathbf{0} & -\mathrm{diag}(\kappa_i)\boldsymbol{I} & \mathbf{0} \\ \mathbf{0} & \mathbf{0} & \mathbf{0} & \eta\,\mathrm{diag}(h_i)\boldsymbol{I} & -\gamma_{\mathrm{H}}\boldsymbol{I} \end{bmatrix} \tag{20}$$

Where $\boldsymbol{I}$ and $\mathbf{0}$ are the identity and null matrices of size M, and $\kappa_i = ((1 - g_i - h_i)\gamma_I + h_i\eta + g_i\alpha)$. We next compute the inverse of the transition matrix

$$\boldsymbol{\Sigma^{-1}} = \begin{bmatrix} -\frac{1}{\delta_{\mathrm{E}}}\boldsymbol{I} & \mathbf{0} & \mathbf{0} & \mathbf{0} & \mathbf{0} \\ -\frac{1}{\delta_{\mathrm{P}}}\boldsymbol{I} & -\frac{1}{\delta_{\mathrm{P}}}\boldsymbol{I} & \mathbf{0} & \mathbf{0} & \mathbf{0} \\ -\frac{(1-f)}{\gamma_{\mathrm{A}}}\boldsymbol{I} & -\frac{(1-f)}{\gamma_{\mathrm{A}}}\boldsymbol{I} & -\frac{1}{\gamma_{\mathrm{A}}}\boldsymbol{I} & \mathbf{0} & \mathbf{0} \\ -f\,\mathrm{diag}(\frac{1}{\kappa_i})\boldsymbol{I} & -f\,\mathrm{diag}(\frac{1}{\kappa_i})\boldsymbol{I} & \mathbf{0} & -\mathrm{diag}(\frac{1}{\kappa_i})\boldsymbol{I} & \mathbf{0} \\ -\frac{f\eta}{\gamma_{\mathrm{H}}}\mathrm{diag}(\frac{h_i}{\kappa_i})\boldsymbol{I} & -\frac{f\eta}{\gamma_{\mathrm{H}}}\mathrm{diag}(\frac{h_i}{\kappa_i})\boldsymbol{I} & \mathbf{0} & -\frac{\eta}{\gamma_{\mathrm{H}}}\mathrm{diag}(\frac{h_i}{\kappa_i})\boldsymbol{I} & -\frac{1}{\gamma_{\mathrm{H}}}\boldsymbol{I} \end{bmatrix} \tag{21}$$

The NGM with large domain can now be found by $\boldsymbol{K_L} = -\boldsymbol{T}\boldsymbol{\Sigma}^{-1}$. However, since we know that each individual who gets infected becomes exposed (E compartment), we focus on the NGM with small domain, $\mathbf{K}_\mathrm{S}$, which only consists of the E compartment [16]. We do this by removing the rows that correspond to the other compartments from T and the columns from Σ^{-1} . We then find:

$$\boldsymbol{K_S} = \tau \left[\left(\frac{1}{\delta_P} + \frac{(1-f)}{\gamma_A} \right) \boldsymbol{\Theta} + \mathrm{diag} \left(\frac{f}{\kappa_i} (1 + \frac{h_i \eta}{\gamma_\mathrm{H}}) \right) \boldsymbol{\Theta} \right].$$

The reproduction number is related to the main eigenvalue of $\boldsymbol{K_S}$, i.e. $R_0 = |\lambda_1|$, and τ is estimated from the main eigenvalue of $\tilde{K}_\mathrm{S} = K_\mathrm{S}/\tau$. Considering the null model parameters ($\tilde{\lambda}_1^0$), we have the expression:

$$\tau = \frac{R_0}{|\tilde{\lambda}_1^0|}. \tag{22}$$

Parameterization of the interventions

Safety zone

We considered the existence of a safety zone to protect a certain fraction, f_S, of the population, mostly those more vulnerable. In practice, this involves dividing the camp in two areas, a "green" zone (denoted g) for the protected population and an "orange" zone (o) for the exposed population. These two populations could interact via a buffer zone, under controlled conditions. Based on our assumption that infectivity in the buffer zone is reduced by 80%, $\hat{\tau} = 0.2\tau$. Each individual in the green zone can interact with a limited number (c_visit) of family members (hereafter "visitors") from the orange zone per day. In some interventions we considered that individuals visiting the buffer zone will have a health check (e.g. temperature measurement), aimed at excluding symptomatic individuals. When the health check is applied, the transmission probability between individuals from the orange zone in the I or H compartments and individuals from the green zone is set to zero.

Although setting up a safety zone implies a reduction in the number of contacts between classes of the green zone and the orange zone, the mean number of contacts that each individual has per day, $\bar{c}_i$, is conserved. Therefore we need to estimate how contacts will be redistributed from individuals from a different zone to individuals living in the same zone. We model this redistribution of the contacts with the parameter ϵ_i:

$$\begin{aligned} \epsilon_i &= \rho c_\mathrm{visit}/\bar{c}_i \quad (i,j \text{ in different zones}) \\ \epsilon_i &= 1 - \rho c_\mathrm{visit}/\bar{c}_i \quad (i,j \text{ in same zone}). \end{aligned}$$

If we assume that visitors are always different, the quantity $f_\mathrm{o,visit} = c_\mathrm{visit} \frac{N_\mathrm{g}}{N_\mathrm{o}}$ is the fraction of the orange population that visits the buffer zone. We define ρ as[1]:

$$\rho = \begin{cases} 1 & \text{if } i \in \mathrm{g} \\ f_\mathrm{o,visit} & \text{if } i \in \mathrm{o} \end{cases}$$

Next, we model the probability of interaction between a member of class i and class j, depending on whether they belong to the same or to different zones. Since interaction is limited to others in the same zone, every individual will have a higher likelihood of interaction with members of the classes staying in the same zone compared to the null model. More specifically, the proportion N_i/N of individuals of class i in the null model will become N_i/N_X with N_X the total number of individuals in zone $X = \{\mathrm{o}, \mathrm{g}\}$. This yields the following values for m_{ij}:

[1] If c_visit is large enough ($c_\mathrm{visit} \approx 28$ contacts per week), this function saturates, because every member of the orange zone would eventually visits the buffer zone:

$$\rho = \begin{cases} 1 & \text{if } i \in \mathrm{g} \\ f_\mathrm{o,visit} \left(1 - \mathrm{H}(f_\mathrm{o,visit} - 1) \frac{f_\mathrm{o,visit} - 1}{f_\mathrm{o,visit}} \right) & \text{if } i \in \mathrm{o} \end{cases}$$

with the Heaviside function $\mathrm{H}(f_\mathrm{o,visit} - 1) = 1$ if $f_\mathrm{o,visit} \geq 1$. We chose values well below this saturation threshold.

$$m_{ij} = \left(\frac{N_i}{N_X}\right)/\left(\frac{N}{N_i}\right) = \frac{N}{N_X} \quad (i,j \text{ in same zone } X)$$
$$m_{ij} = \left(\frac{N_i}{N_Y}\right)/\left(\frac{N}{N_i}\right) = \frac{N}{N_Y} \quad (i \in X \text{ and } j \in Y).$$

We finally define the management matrix as $M_{ij} = \epsilon_i m_{ij}$.

Estimation of the infectivity of the isolated and evacuated populations

To estimate the infectivity of the isolated population, we make the following assumptions. We considered a number N_{care} of carers having c_{care} contacts per day with the isolated population. Carers are entirely drawn from younger adults (age 2) with no comorbidities, and must have no symptoms. We denote the number of individuals fulfilling these requirements with N_{exp} (number of exposed). When the number of symptomatic individuals exceeds the isolation capacity, $\tilde{N}$, the individuals in excess are fully infectious (note that we use a tilde to denote variables related to the isolated population). In addition, the occupancy of the isolation beds is distributed among classes proportionally to the number of symptomatic individuals present in each class, i.e. $\tilde{N}_j = \tilde{N}\left(I_j/\sum_j I_j\right)$. Finally, symptomatic individuals developing symptoms that would require hospitalization, are either evacuated or become fully infectious. The rationale behind the latter choice is that camps lack the necessary means to adequately protect the rest of the population when individuals require more dedicated care. In particular, it is unlikely that a severely ill individual would be able to stay alone in a tent. We model evacuation considering a parameter $\epsilon = 0$ if evacuation is put in place and $\epsilon = 1$ otherwise. Evacuated individuals are no longer infectious.

Given these assumptions, the number of contacts that the healthy younger adult population class will have with the isolated population will be $c_{\text{care}}N_{\text{care}}/N_{\text{exp}}$ per individual and day. The expression clearly shows that increasing the number of carers, the number of isolated individuals, and the number of contacts per day between carers and individuals, will increase the rate of infection. Hence, we expect that for fixed N_{care} and c_{care}, the positive effects of isolation will be diminished as $\tilde{N}$ increases. We further assume that this interaction will be regulated through a buffer zone, so infectivity is reduced by 80%, denoted by $\xi = 0.2$. Finally, we note that the probability of finding an isolated individual belonging to class j, is equal to $(N_j/N)(\tilde{N}_j/N_j)$, but this probability is equal to one for the healthy younger adult population (due to their role as carers) and zero for the remaining classes (since they have no access to the isolation area).

For simplicity, we assume that there is one carer for each infected person in the class j, ($N_{\text{care},j} = \tilde{N}_j$), having only one contact per day (c_{care}). Note the convenience of this choice, since if the number of symptomatic individuals is larger than the number of potential carers, the ratio $\tilde{N}_j/N_{\text{exp}} > 1$, implying more than one contact per day is needed to take care of that population class. With these considerations, the rate of infection for the healthy younger adult population class (indexed k) becomes:

$$\lambda_k = \tau \sum_j \xi \frac{\tilde{N}_j}{N_{\text{exp}}} + C_{kj}\frac{P_j + A_j + \Theta(N_I - \tilde{N})(I_j - \tilde{I}_j) + \epsilon H_j}{N_j},$$

where Θ is the Heaviside function and N_I the total number of symptomatic individuals at time t. For the remaining classes ($i \neq k$) the rate of infection becomes:

$$\lambda_i = \tau \sum_j C_{ij}\frac{P_j + A_j + \Theta(N_I - \tilde{N})(I_j - \tilde{I}_j) + \epsilon H_j}{N_j}.$$

A final consideration is that symptomatic individuals require some time to recognize their symptoms and to self-isolate. To model this, whenever simulating the isolation intervention, the symptomatic compartment is split in two compartments: onset of symptoms, I_i^{onset}, and symptomatic, I_i. We assumed the duration of I_i^{onset} follows a Gaussian distribution with means 12, 24 or 48 hours on average. The duration for which an individual isolates is then calculated as the difference between the symptomatic period if there is no isolation and the duration spent in the symptom onset compartment.

Supplementary figures

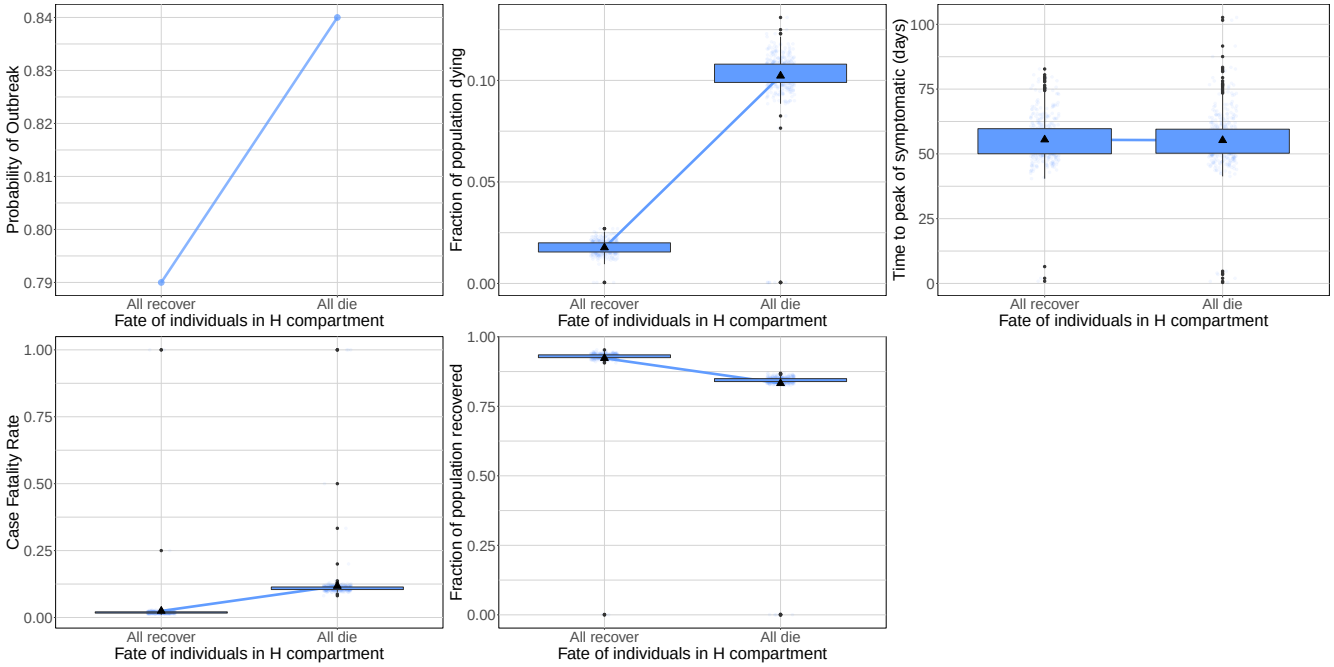

Figure 2: **Outcomes when all severe cases recover vs when all severe cases die.** Probability of an outbreak (top left), fraction of the population dying (top middle), time until peak symptomatic cases (top right), CFR (bottom left), and fraction of the population that recovers (bottom middle).

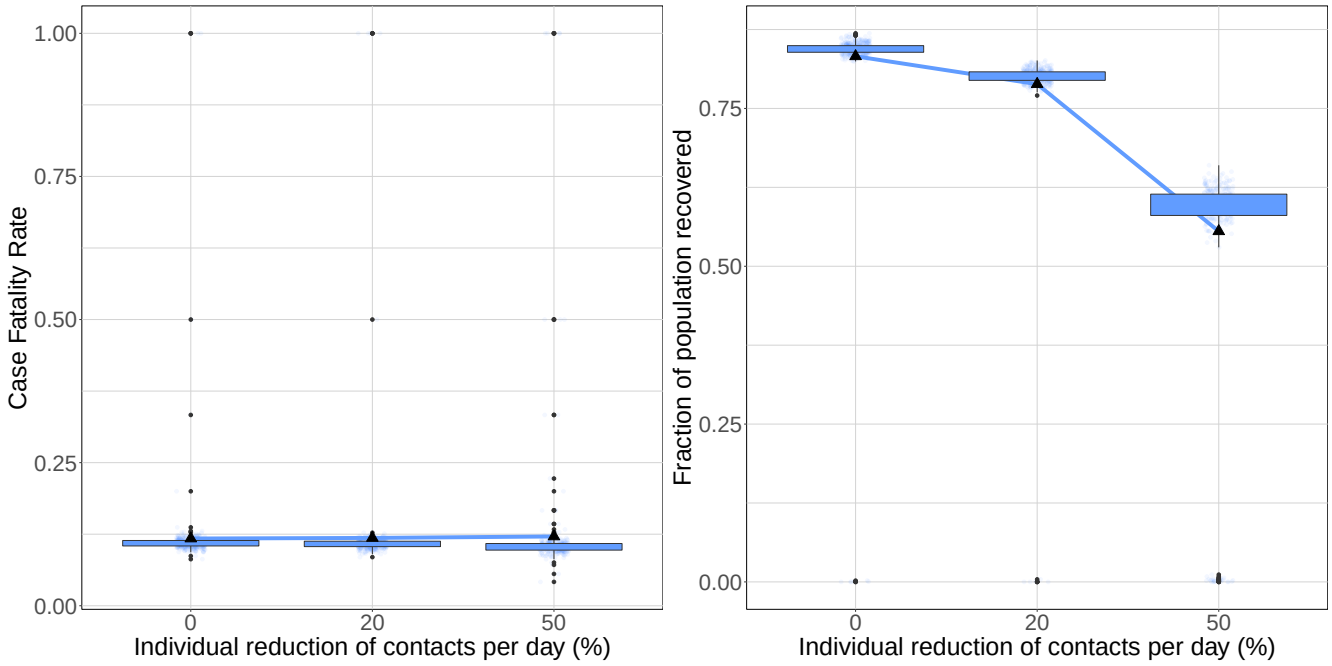

Figure 3: **Self-distancing.** CFR (left), and fraction of the population that recovers (right) as a function of the proportion of contacts reduced per individual per day.

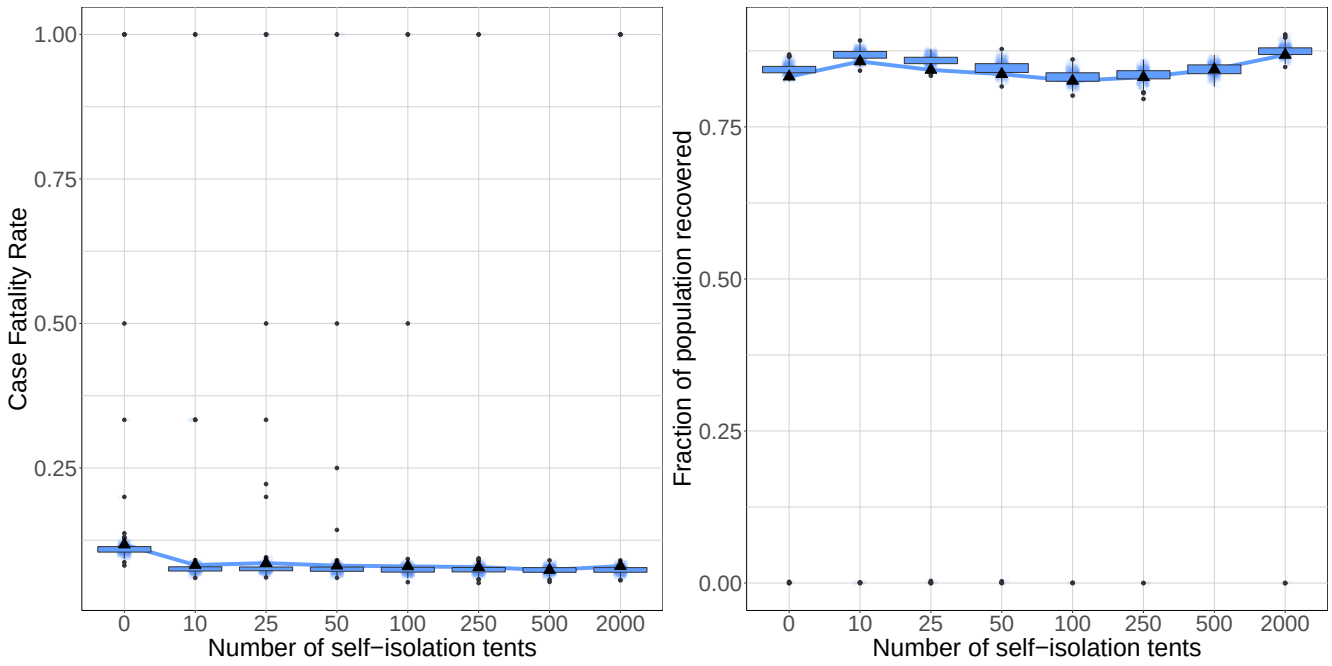

Figure 4: **Self-isolation.** CFR (left), and fraction of the population that recovers (right) as a function of the number of isolation tents available in the camp.

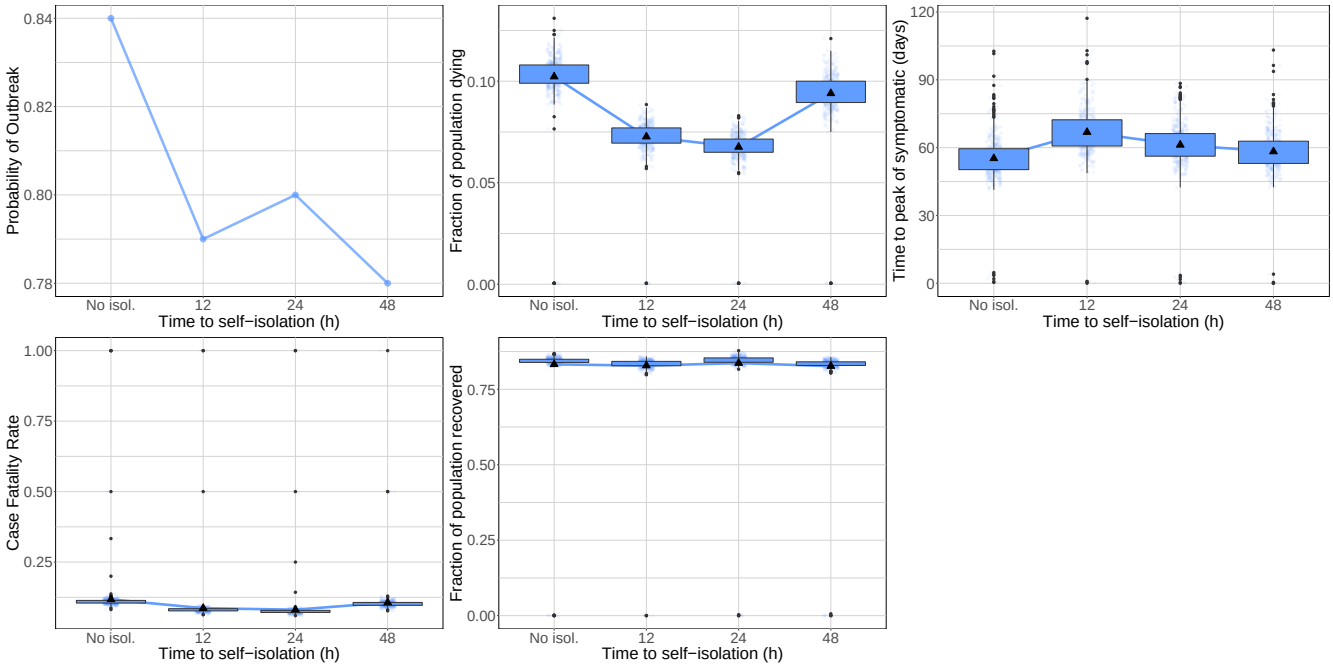

Figure 5: **Time to self-isolation.** Probability of an outbreak (top left), fraction of the population dying (top middle), time until peak symptomatic cases (top right), CFR (bottom left), and fraction of the population that recovers (bottom middle) as a function of the time that individuals require to recognize their symptoms and self-isolate.

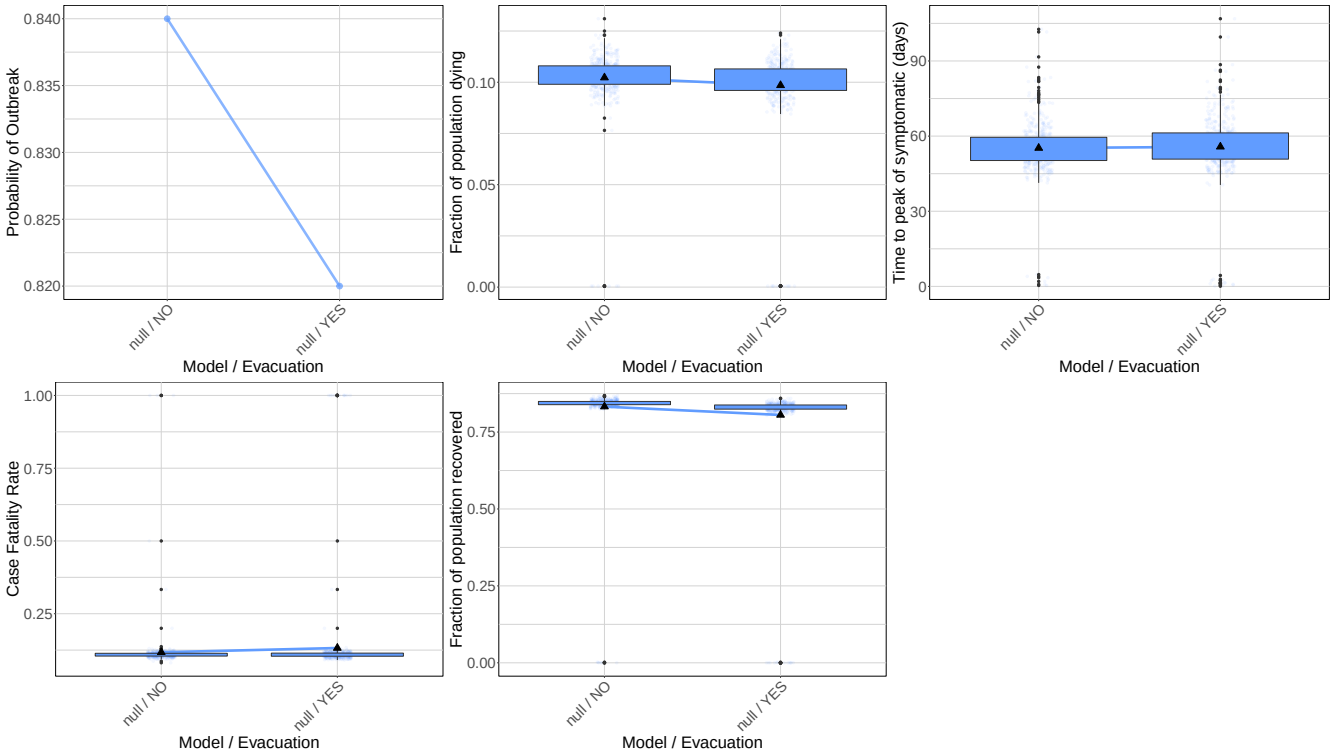

Figure 6: **Evacuation.** Probability of an outbreak (top left), fraction of the population dying (top middle), time until peak symptomatic cases (top right), CFR (bottom left), and fraction of the population that recovers (bottom middle), as a function of whether individuals requiring hospitalization are evacuated to isolation centers.

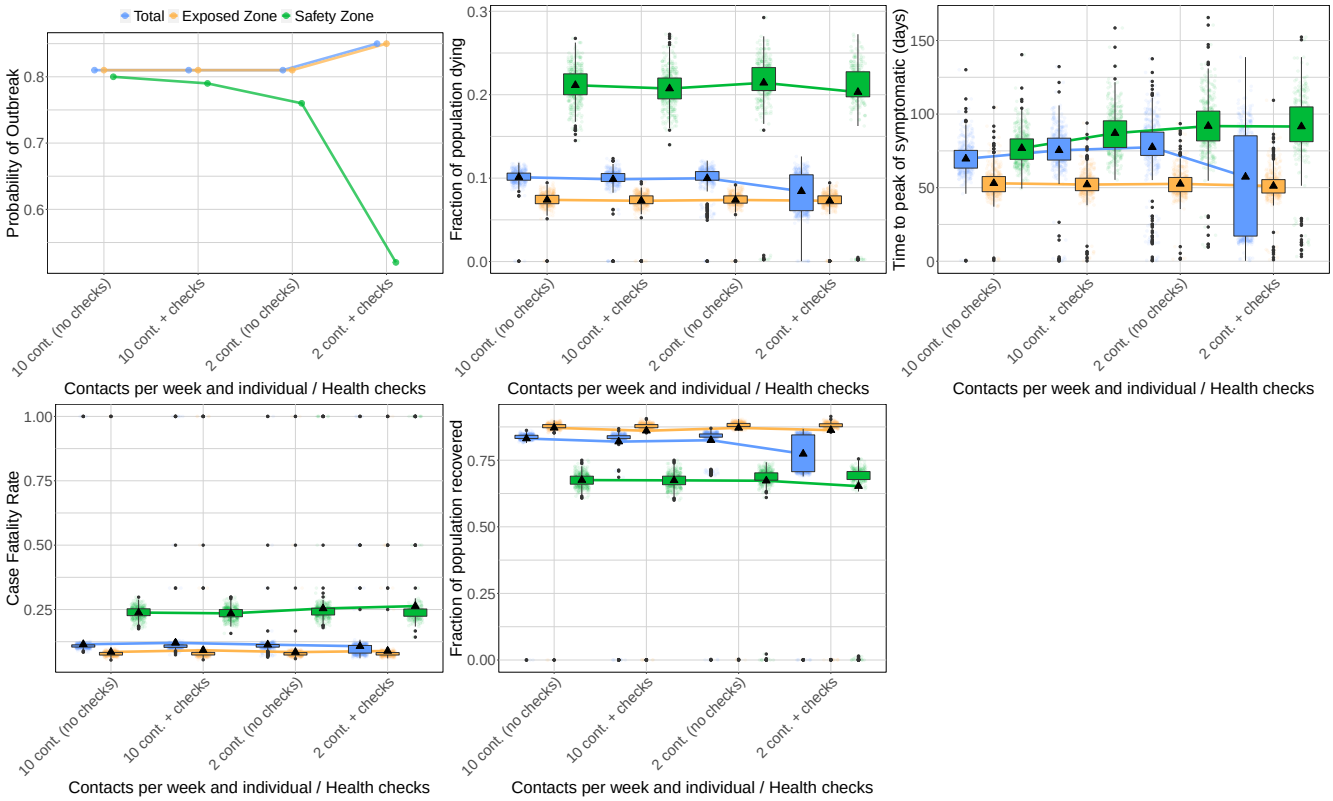

Figure 7: **Health-checks in the buffer zone.** Probability of an outbreak (top left), fraction of the population dying (top middle), time until peak symptomatic cases (top right), CFR (bottom left), and fraction of the population that recovers (bottom middle), as a function of whether health-checks are implemented in the buffer zone between the safety and exposed zones. Scenarios with 10 or 2 contacts in the buffer zone per person in the safety zone per week are plotted. All figures consider the scenario in which 20% of the camp's population is allocated to the safety zone.

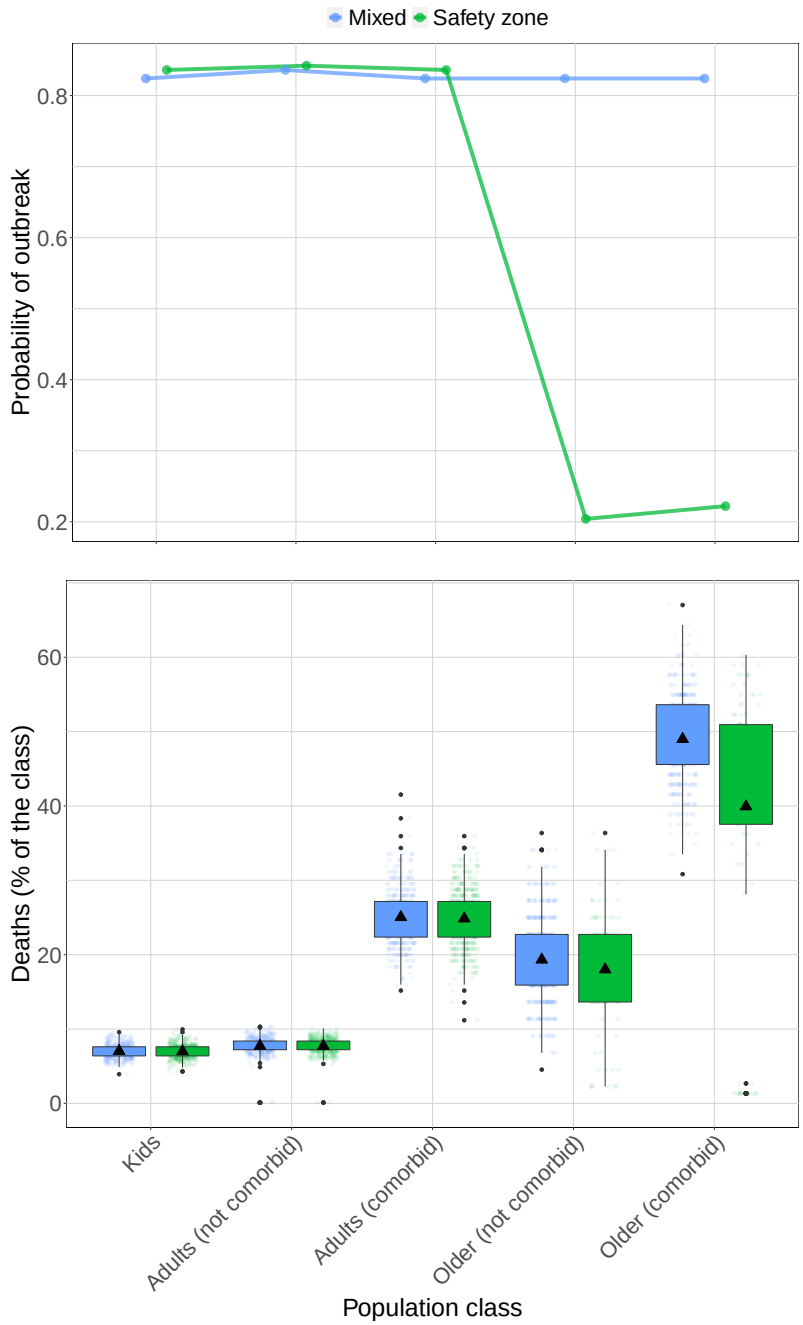

Figure 8: **Effects of the safety zone on outcomes by population class.** Probability of an outbreak (top), and proportion that dies in each population class (bottom) when no interventions are implemented (Mixed), compared to protection of older adults in the safety zone with 2 contacts in the buffer zone per week (Safety zone). The fraction of deaths in the safety zone for the older population is significantly lower (Kruskal-Wallis test, p-val$< 10^{-15}$).

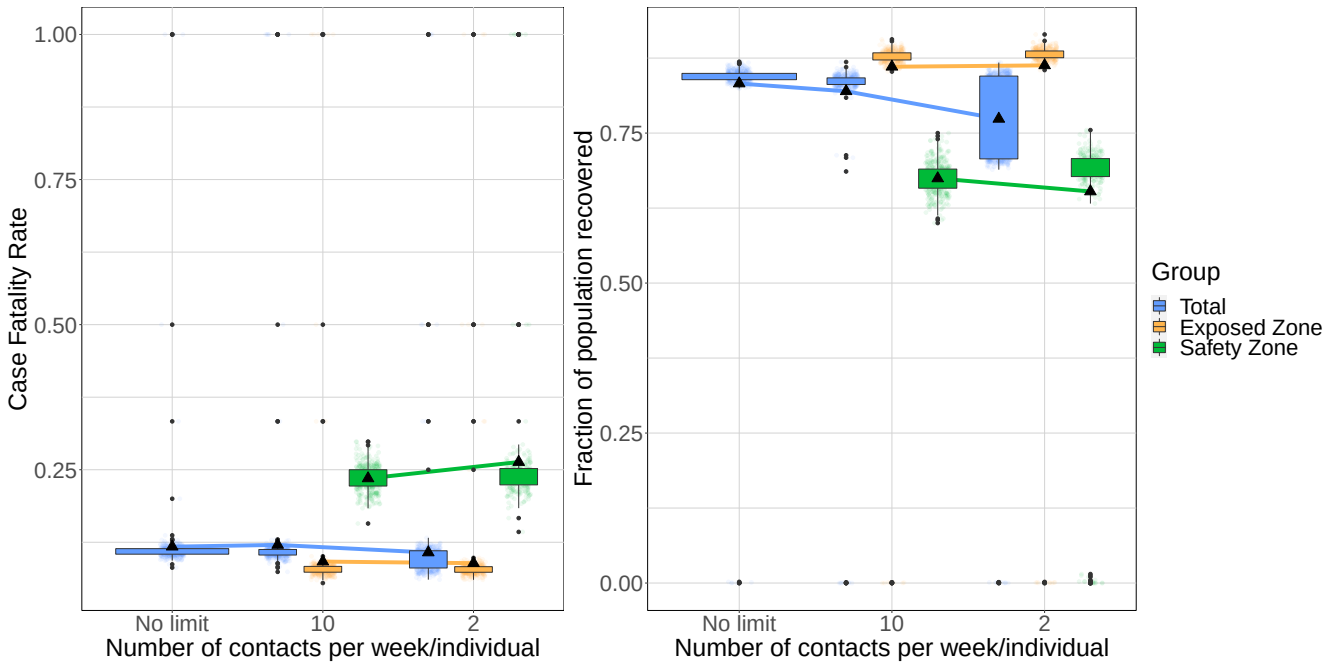

Figure 9: **Number of contacts in the buffer zone.** CFR (left), and fraction of the population that recovers (right) as a function of the number of contacts that each individual in the safety zone has in the buffer zone per week. All figures consider the scenario in which 20% of the camp's population is allocated to the safety zone.

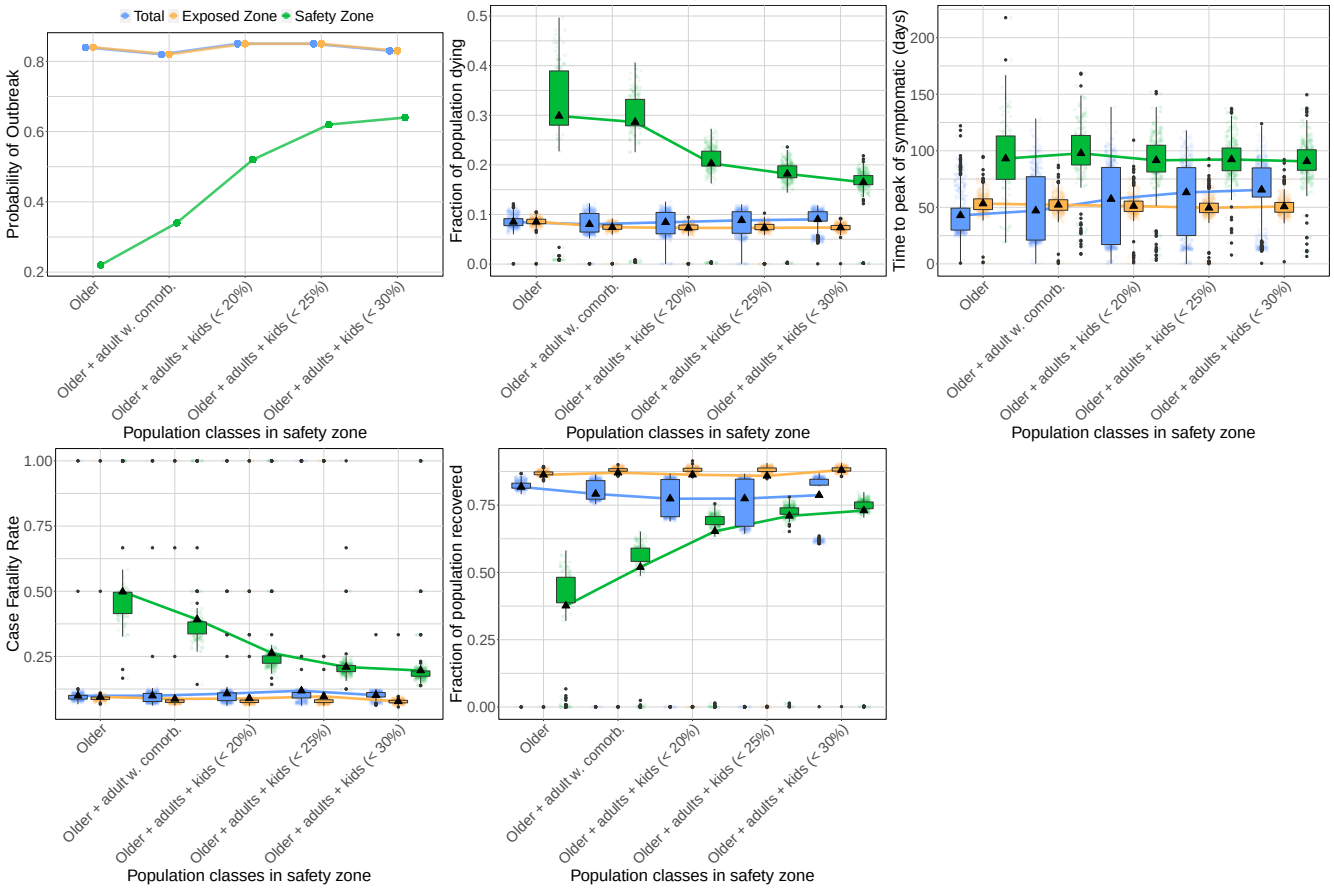

Figure 10: **Population moving to the safety zone.** Probability of an outbreak (top left), fraction of the population dying (top middle), time until peak symptomatic cases (top right), CFR (bottom left), and fraction of the population that recovers (bottom middle) as a function of the safety zone allocation scenario (see Table 3). All figures consider the scenario with 2 contacts in the buffer per person in the safety zone per week.

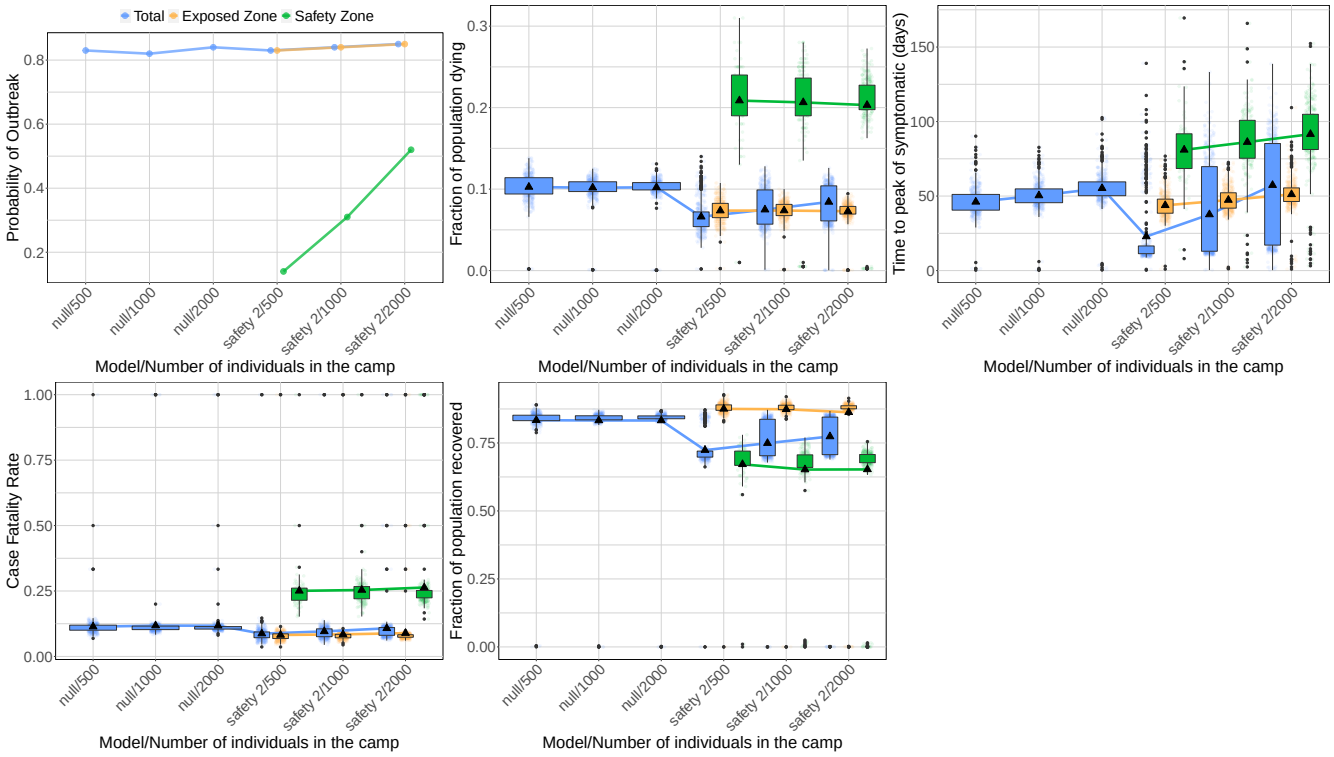

Figure 11: **Efficacy of the safety zone for different population sizes.** Probability of an outbreak (top left), fraction of the population dying (top middle), time until peak symptomatic cases (top right), CFR (bottom left), and fraction of the population that recovers (bottom middle) as a function of the total population size. The figures consider scenarios with no interventions (null), and with a safety zone comprising 20% of the camp's population with 2 contacts in the buffer zone per person in the safety zone per week (safety 2).

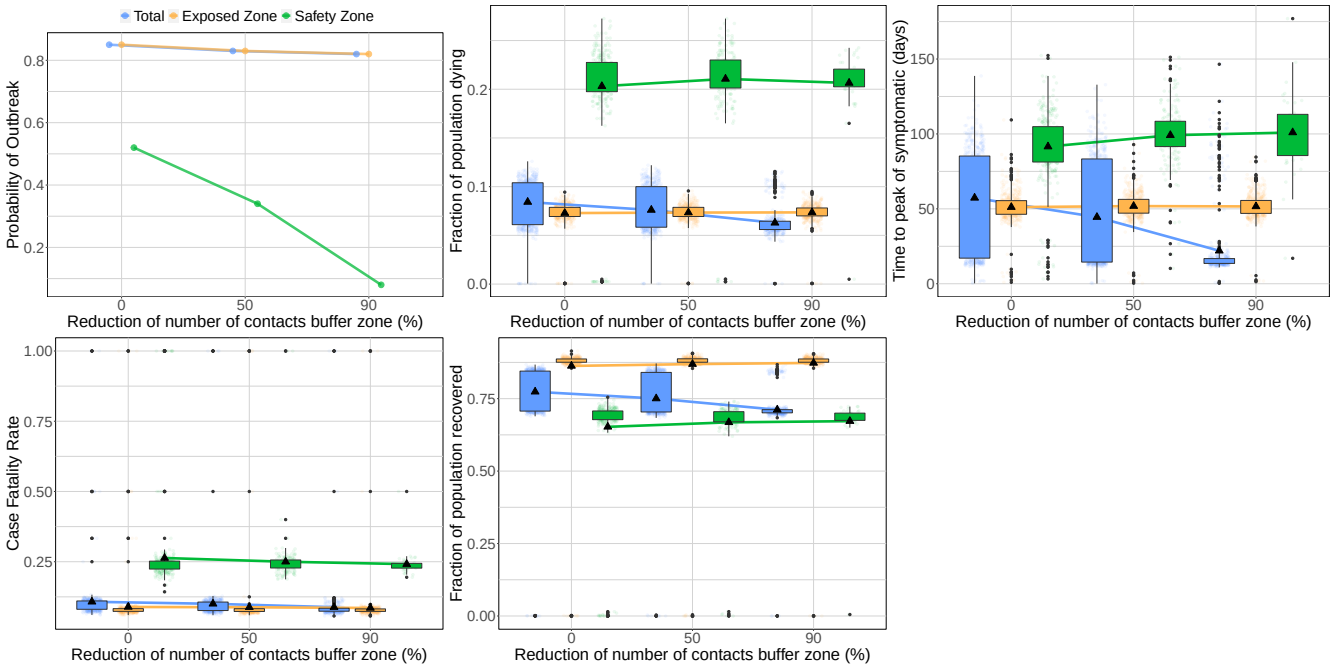

Figure 12: **Lockdown of the safety zone.** Probability of an outbreak (top left), fraction of the population dying (top middle), time until peak symptomatic cases (top right), CFR (bottom left), and fraction of the population that recovers (bottom middle) as a function of the reduction in the number of contacts permitted in the buffer zone from a baseline of 2 per person in the safety zone per week. All figures consider the scenario in which 20% of the camp's population is allocated to the safety zone.

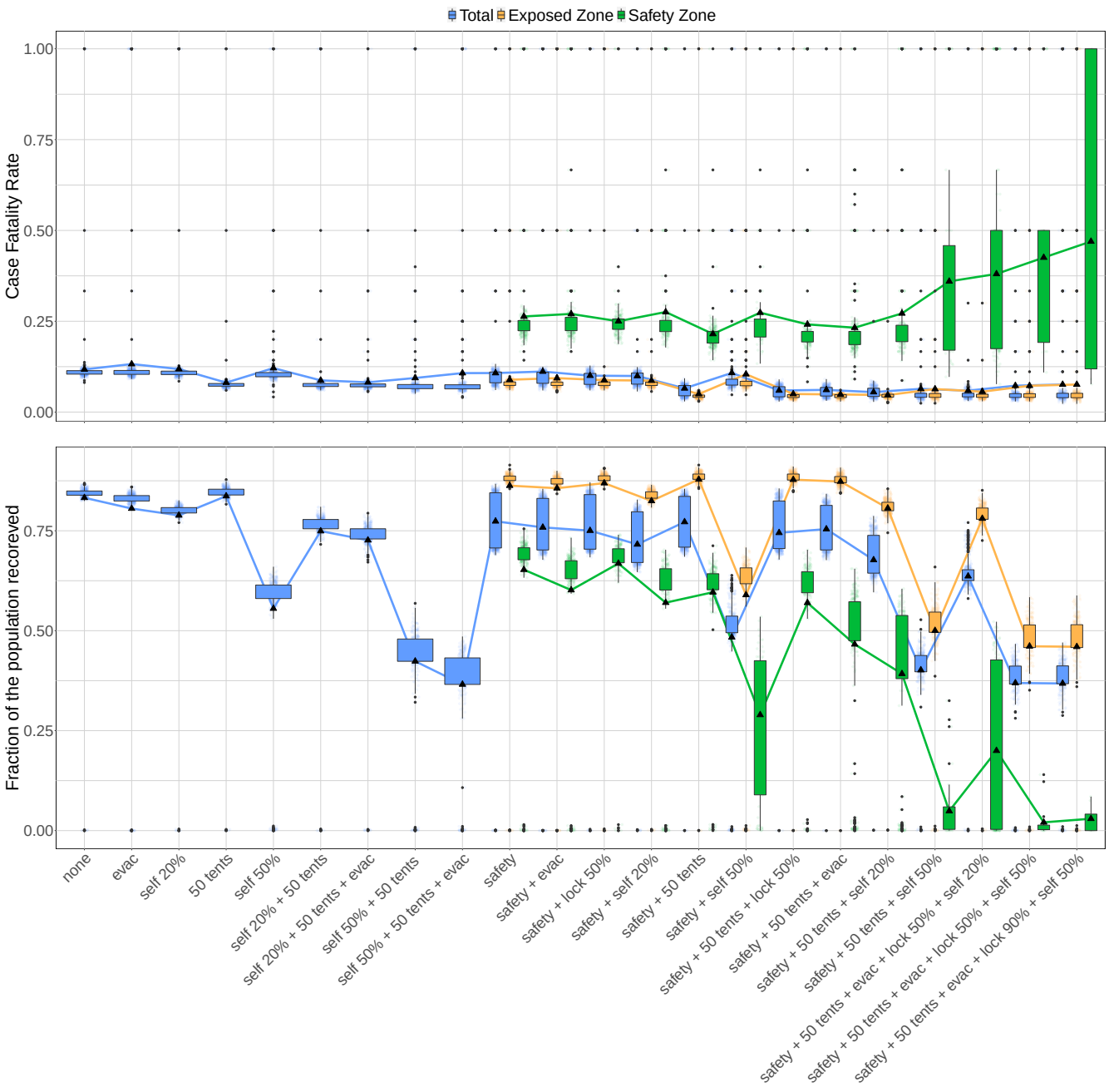

Figure 13: **Combined interventions.** CFR (top), and fraction of the population that recovers (bottom) for different combinations of interventions. Evac = evacuation of severely symptomatic, self = self-distancing, tents = number of available self-isolation tents, safety = safety zone, lock = lockdown of the buffer zone. For combinations of interventions including a safety zone, we distinguish between the population living in the green zone, in the orange zone and the whole population. The increase in the CFR for the green zone is explained by the discretization of the possible values that the CFR can take when the number of cases is very low (see Supplementary Table 4).

Intervention	<20 cases	Total	% of total
safety	16	270	5.9
safety + evac	20	249	8
safety + lock 50%	5	171	2.9
safety + self 20%	19	188	10
safety + 50 tents	11	240	4.6
safety + self 50%	14	64	22
safety + 50 tents + lock 50%	14	154	9.1
safety + 50 tents + evac	33	239	14
safety + 50 tents + self 20%	31	144	22
safety + 50 tents + self 50%	25	38	66
safety + 50 tents + evac + lock 50% + self 20%	53	110	48
safety + 50 tents + evac + lock 50% + self 50%	18	20	90
safety + 50 tents + evac + lock 90% + self 50%	6	8	75

Table 4: **Efficacy of the safety zone in combination with other interventions.** <20 cases = number of outbreaks in the green zone with fewer than 20 cases recorded. Total = total number of simulations where an outbreak in the green zone occurs (at least one death). % of total = percent of outbreaks where fewer than 20 cases are recorded. N = 500 simulations for each combination of interventions. For the most effective combinations, the majority of simulations where an outbreak occurs in the green zone see fewer than 20 cases. In these simulations, the discretization of the possible values that the CFR can take explains its apparently anomalous increase in Fig. 13.

References

[1] Shannon Doocy, Emily Lyles, Baptiste Hanquart, Michael Woodman, and The LHAS Study Team. Prevalence, care-seeking, and health service utilization for non-communicable diseases among Syrian refugees and host communities in Lebanon. *Conflict and Health*, 10(1):21, October 2016.

[2] Shannon Doocy, Emily Lyles, Timothy Roberton, Laila Akhu-Zaheya, Arwa Oweis, and Gilbert Burnham. Prevalence and care-seeking for chronic diseases among Syrian refugees in Jordan. *BMC Public Health*, 15(1):1097, October 2015.

[3] Assistance Coordinator Unit. The Syrian IDP camps monitoring study - Northern Syria camps - Humanitarian Data Exchange. url: https://data.humdata.org/dataset/idp-camps-monitoring-november-of-2018.

[4] Yuanyuan Dong, Xi Mo, Yabin Hu, Xin Qi, Fang Jiang, Zhongyi Jiang, and Shilu Tong. Epidemiological characteristics of 2143 pediatric patients with 2019 coronavirus disease in china. *Pediatrics*, 2020.

[5] CDC Covid, CDC COVID, CDC COVID, Nancy Chow, Katherine Fleming-Dutra, Ryan Gierke, Aron Hall, Michelle Hughes, Tamara Pilishvili, Matthew Ritchey, et al. Preliminary estimates of the prevalence of selected underlying health conditions among patients with coronavirus disease 2019 in usa, february 12–march 28, 2020. *Morbidity and Mortality Weekly Report*, 69(13):382, 2020.

[6] Qun Li, Xuhua Guan, Peng Wu, Xiaoye Wang, Lei Zhou, Yeqing Tong, Ruiqi Ren, Kathy SM Leung, Eric HY Lau, Jessica Y Wong, et al. Early transmission dynamics in wuhan, china, of novel coronavirus–infected pneumonia. *New England Journal of Medicine*, 2020.

[7] Xi He, Eric HY Lau, Peng Wu, Xilong Deng, Jian Wang, Xinxin Hao, Yiu Chung Lau, Jessica Y Wong, Yujuan Guan, Xinghua Tan, et al. Temporal dynamics in viral shedding and transmissibility of covid-19. *Nature medicine*, 26(5):672–675, 2020.

[8] Peter Ashcroft, Jana S. Huisman, Sonja Lehtinen, Judith A. Bouman, Christian L. Althaus, Roland R. Regoes, and Sebastian Bonhoeffer. COVID-19 infectivity profile correction. *arXiv:2007.06602 [q-bio, stat]*, July 2020. arXiv: 2007.06602.

[9] Roman Wölfel, Victor M Corman, Wolfgang Guggemos, Michael Seilmaier, Sabine Zange, Marcel A Müller, Daniela Niemeyer, Terry C Jones, Patrick Vollmar, Camilla Rothe, et al. Virological assessment of hospitalized patients with covid-2019. *Nature*, 581(7809):465–469, 2020.

[10] Dawei Wang, Bo Hu, Chang Hu, Fangfang Zhu, Xing Liu, Jing Zhang, Binbin Wang, Hui Xiang, Zhenshun Cheng, Yong Xiong, et al. Clinical characteristics of 138 hospitalized patients with 2019 novel coronavirus–infected pneumonia in wuhan, china. *Jama*, 323(11):1061–1069, 2020.

[11] Oyungerel Byambasuren, Magnolia Cardona, Katy Bell, Justin Clark, Mary-Louise McLaws, and Paul Glasziou. Estimating the extent of true asymptomatic covid-19 and its potential for community transmission: systematic review and meta-analysis. *Available at SSRN 3586675*, 2020.

[12] Jennifer Harcourt, Azaibi Tamin, Xiaoyan Lu, Shifaq Kamili, Senthil K Sakthivel, Janna Murray, Krista Queen, Ying Tao, Clinton R Paden, Jing Zhang, et al. Severe acute respiratory syndrome coronavirus 2 from patient with coronavirus disease, united states. *Emerging infectious diseases*, 26(6):1266, 2020.

[13] O. Diekmann, Hans Heesterbeek, and Tom Britton. *Mathematical tools for understanding infectious diseases dynamics*. Princeton series in theoretical and computational biology. Princeton University Press, Princeton, 2013.

[14] Sydney Philipps, Dan Rossi, Rachel Von Arb, and Alex Capaldi. Mathematical models of infectious diseases: Two-strain infections in metapopulations, July 2011.

[15] Marino Gatto, Enrico Bertuzzo, Lorenzo Mari, Stefano Miccoli, Luca Carraro, Renato Casagrandi, and Andrea Rinaldo. Spread and dynamics of the COVID-19 epidemic in Italy: Effects of emergency containment measures. *Proceedings of the National Academy of Sciences*, 117(19):10484–10491, May 2020.

[16] J.M Heffernan, R.J Smith, and L.M Wahl. Perspectives on the basic reproductive ratio. *Journal of the Royal Society Interface*, 2(4):281–293, sep 2005.